Proceedings of the International Conference on Oxide Materials for Electronic Engineering, May 29–June 2, 2017, Lviv

Water-Sorption Effects near Grain Boundaries in Modified MgO–Al_2O_3 Ceramics Tested with Positron–Positronium Trapping Algorithm

H. Klym[a,*], A. Ingram[b], O. Shpotyuk[c,d,e], I. Hadzaman[f] and D. Chalyy[g]

[a]Lviv Polytechnic National University, 12 Bandery Str., Lviv, 79013, Ukraine

[b]Opole University of Technology, Ozimska 75, 45-370 Opole, Poland

[c]Vlokh Institute of Physical Optics, 23 Dragomanova Str., Lviv, 79005, Ukraine

[d]Jan Dlugosz University of Czestochowa, al. Armii Krajowej 13/15, 42-201 Czestochowa, Poland

[e]Scientific Research Company "Carat", 202 Stryjska Str., Lviv, 79031, Ukraine

[f]Drohobych Ivan Franko State Pedagogical University, 24 I. Franko Str., Drohobych, 82100, Ukraine

[g]Lviv State University of Life Safety, 35 Kleparivska Str., Lviv, 79000, Ukraine

Water-sorption processes near grain boundaries in the MgO–Al_2O_3 ceramics prepared at different temperatures were studied using positron annihilation lifetime spectroscopy. Numerical values of three- and four-component treatment of spectra were used for study of physical- and chemical-sorption processes in the MgO–Al_2O_3 ceramics. To apply mathematical approach in the form of positron–positronium trapping algorithm into three-component treatment of positron annihilation lifetime spectra it was shown that physical-adsorbed water did not modify positron trapping sites near grain boundaries in water-immersed MgO–Al_2O_3 ceramics and localized mainly in nanopores. The chemically-adsorbed water modifies structural extended defects located near grain boundaries that accompanied them by void fragmentation at water desorption.

DOI: 10.12693/APhysPolA.133.864

PACS/topics: 81.05.Je, 07.07.Df

1. Introduction

Humidity-sensitive MgO–Al_2O_3 ceramics are well-known materials with extended porous structure providing their wide functional applications [1–3]. These ceramics are stable in comparison with other porous functional materials possessing rapid response to humidity changes [4]. These changes provide by microstructure of grains, grain boundaries and pores (or free-volume entities) in ceramic materials [5, 6].

Influence of initial surface area of initial components (MgO and Al_2O_3) on the structural properties of MgO–Al_2O_4 ceramics prepared at 1100–1400 °C was studied early in [7–10]. As was established in [11], structural properties of spinel ceramics depend on their sintering temperature and duration. Structure of humidity-sensitive MgO–Al_2O_3 ceramics is improved with the increase of sintering temperature, which mainly results in the transformation of pore size distribution and decrease of amount of MgO/Al_2O_3 phases located near grain boundaries. Evolution of pore size distribution (increases of amount and quantity of open micro-, macro- and nanopores) in humidity-sensitive spinel ceramics leads to better water-adsorption and desorption processes with minimal hysteresis of exploitation characteristics in these materials [7, 11].

*corresponding author; e-mail: klymha@yahoo.com

Porous structure of functional materials are studied using traditional methods such as X-ray diffraction, electron microscopy and different porosimetry methods, etc. [12, 13]. However, porosimetry techniques provide information on open pores with radii over 2 nm [13], whereas processes of capillary condensation in such ceramics depend also on nanopores smaller than 2 nm [14].

To study such small nanopores and free volumes in ceramic structure we used the method of positron annihilation lifetime (PAL) spectroscopy, which is alternative tool of structural characterization of open and closed nanopores [15]. Two channels of positron annihilation were shown to be important in case of ceramics: positron trapping (two components) and *ortho*-positronium (*o*-Ps) decaying (one or two components) [16]. In general, these two channels of positron annihilation are independent. However, if trapping sites will appear in a vicinity of grain boundaries neighboring with free-volume pores, these positron–positronium traps become mutually interconnected resulting in a significant complication of PAL data. This occurs provided the input of one of the above annihilation channels will be significantly changed. In addition, adsorbed water influences on processes of physical and chemical adsorption of water near grain boundaries in the MgO–Al_2O_3 ceramics.

Early we used PAL method to study influence of sintering conditions in the MgO–Al_2O_3 ceramics in general (to characterization of MgO–Al_2O_3 ceramics sintered at 1100–1400 °C) and water-sorption processes in nanopores of these materials (at analysis of third and fourth com-

ponents of PAL spectra) [10, 17]. In this work, to clarify this feature, we shall analyze physical water-sorption process near grain boundaries in the modified $MgO–Al_2O_3$ ceramics using positron–positronium trapping algorithm proposed in [18] (at interpretation of three-component treatment of PAL spectra) in comparison with chemical water-sorption process at decomposition of PAL spectra into four components.

2. Experimental

The modified $MgO–Al_2O_3$ ceramics were prepared using traditional ceramic route at maximal temperatures (T_s) of 1100–1400 °C during 2 h as it was described in [7–11, 17, 19]. In respect to X-ray diffraction measurements [7], the ceramics prepared at lower T_s = 1100–1200 °C are composed of main spinel phase and large amount of additional MgO and Al_2O_3 phases (up to 12%), while the ceramics sintered at high T_s of 1300 °C and 1400 °C contain additionally only MgO phase in the amount of 3.5 and 1.5%, respectively.

The PAL measurements were performed with the ORTEC instrument (^{22}Na source) [17]. The first experiment were performed at 22 °C and relative humidity RH = 35% after immersion of ceramic samples into distillated water for 12 h. Then, the PAL measurements were repeated once more with water-immersed ceramics at the same conditions. In the second case PAL measurement for ceramic samples was carried out at 22 °C and relative humidity RH= 35% after 1 day of water exposure (water wetting in distiller at RH = 100%) and drying in a vacuum at 120 °C during 4 h [17].

Each PAL spectrum was collected to analyze short and intermediate PAL components. Further processing of PAL spectra was performed with LT 9.0 program [20] considering the three- or four-component treatment [7, 17, 21]. In spinel ceramics the lifetime τ_2 is related to the size of free-volume defects (or voids) near grain boundaries, and I_2 intensity reflects their amount [17]. The third and fourth components (τ_3, I_3) and (τ_4, I_4) originate from annihilation of *o*-Ps atoms in intrinsic nanopores of $MgO–Al_2O_3$ ceramics. Using positron trapping parameters, the positron trapping modes (average positron lifetimes τ_{av}, positron lifetime in defect-free bulk τ_b and positron trapping rate in defects κ_d) were calculated within two-state positron trapping model [9, 22].

The effects caused by physical-adsorbed water in modified $MgO–Al_2O_3$ ceramics were studied using the positron–positronium trapping algorithm detail described in [18] (in the case of three-component treatment of PAL spectra). This method is a test-indicator in terms of transformation of positronium sites in the initial $MgO–Al_2O_3$ matrix towards positron trapping sites in $MgO–Al_2O_3$ ceramics with absorbed water. In respect to algorithm described in [18], physical parameterization water-related sites can be finally performed taking (τ_{int}, I_{int}) as corresponding components of the generalized two-term decomposed PAL spectrum of a substance affected by embedded water immersion.

3. Results and discussion

Typical PAL spectra reconstructed on three components for modified $MgO–Al_2O_3$ ceramics prepared at 1400 °C are shown in Fig. 1. As it was established early in [7, 11] the $MgO–Al_2O_3$ ceramics are characterized by good adsorption capacity, which is provided by branched porous structure and specificity formation of grains and grain boundaries. But desorption processes in ceramics are more interesting to investigation, since part of absorbed water remains in the internal structure of material localized near grain boundaries and in small nanopores. Schematic cut-section diagram illustrating water-adsorption processes in ceramics is shown in Fig. 2.

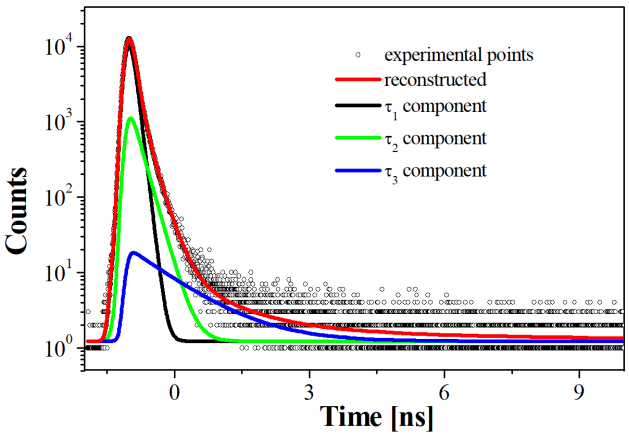

Fig. 1. PAL spectra of $MgO–Al_2O_3$ ceramics sintered at 1400 °C reconstructed from three-component fitting at the general background of source contribution (bottom inset shows statistical scatter of variance).

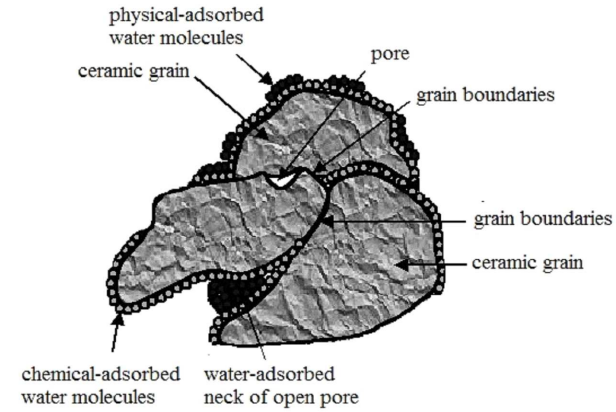

Fig. 2. Schematic cut-section diagram illustrating water-adsorption processes on ceramics.

Positron trapping parameters and modes in "dry" (investigated at 20 °C and 35% of relative humidity) and "immersed" ceramics sintered at different T_s is shown in Table I. It is established that the third largest component is affected by the biggest changes. The filling of nanopores of ceramics by water is manifested in increase of intensity I_3 from 0.02 to 0.12–0.15, which reflects more intense annihilation of *o*-Ps in nanopores filled by water.

The positron trapping parameters caused by residual water (or humidity) were estimated using the positron–positronium trapping algorithm, early used to study evolution of voids in Ge–Ga–Se glasses caused by their "cold" crystallization [23]. Water-immersed ("immersed") MgO–Al_2O_3 ceramics sintered at different T_s were taken as modified matrix and "dry" ceramics sintered at the same temperatures — as initial matrix. Comparative analysis parameters of own positron trapping and corresponding parameters for modified matrix is shown in Table II.

TABLE I

Fitting parameters and positron trapping modes for "dry" and "immersed" sample of MgO–Al_2O_3 ceramics sintered at different T_s

T_s [°C]	Matrix pre-history	Fitting parameters						Positron trapping modes		
		τ_1 [ns]	I_1 [a.u.]	τ_2 [ns]	I_2 [a.u.]	τ_3 [ns]	I_3 [a.u.]	$\tau_{av.}$ [ns]	τ_b [ns]	κ_d [ns^{-1}]
1100	"dry"	0.24	0.68	0.50	0.30	2.59	0.02	0.320	0.285	0.663
	"immersed"	0.24	0.56	0.50	0.29	1.88	0.15	0.329	0.292	0.739
1200	"dry"	0.23	0.70	0.47	0.28	2.39	0.02	0.299	0.269	0.634
	"immersed"	0.23	0.59	0.48	0.28	1.88	0.13	0.310	0.276	0.729
1300	"dry"	0.22	0.72	0.44	0.26	2.19	0.02	0.278	0.254	0.603
	"immersed"	0.22	0.54	0.46	0.32	1.88	0.15	0.309	0.273	0.882
1400	"dry"	0.19	0.76	0.36	0.22	1.90	0.02	0.228	0.213	0.558
	"immersed"	0.21	0.56	0.43	0.32	1.94	0.12	0.290	0.258	0.886

TABLE II

Comparison of own positron trapping parameters with corresponding parameters for the modified ("dry") matrix of MgO–Al_2O_3 ceramics (calculated within positron–positronium trapping algorithm)

T_s, ^{O}Ń	Fitting parameters and positron trapping modes for modified ("dry") matrix					Own positron trapping parameters and modes				
	τ_2 [ns]	I_2 [a.u.]	$\tau_{av.}$ [ns]	τ_b [ns]	κ_d [ns^{-1}]	τ_{int} [ns]	I_{int} [a.u.]	$\tau_{av.}$ [ns]	τ_b [ns]	κ_d [ns^{-1}]
1100	0.50	0.30	0.32	0.28	0.60	0.500	0.261	0.320	0.285	0.667
1200	0.47	0.28	0.30	0.27	0.60	0.468	0.237	0.298	0.269	0.637
1300	0.44	0.26	0.27	0.25	0.60	0.436	0.217	0.277	0.253	0.607
1400	0.36	0.22	0.24	0.20	0.60	0.338	0.167	0.217	0.203	0.582

TABLE III

Positron trapping parameters and modes for "water-wetted" and "dried" MgO–Al_2O_3 ceramics sintered at different T_s

Matrix pre-history	τ_1 [ns]	I_1, [a.u.]	τ_2 [ns]	I_2 [a.u.]	τ_3 [ns]	I_3 [a.u.]	τ_4 [ns]	I_4 [a.u.]	$\tau_{av.}$ [ns]	τ_b [ns]	κ_d [ns^{-1}]
1100 °C											
"water-wetted"	0.17	0.66	0.48	0.28	1.820	0.044	53.05	0.009	0.263	0.21	1.15
"dried"	0.17	0.68	0.45	0.29	2.215	0.021	68.29	0.019	0.257	0.21	1.08
1200 °C											
"water-wetted"	0.17	0.64	0.42	0.31	2.047	0.038	58.67	0.004	0.252	0.21	1.19
"dried"	0.16	0.72	0.43	0.23	2.290	0.031	68.87	0.017	0.229	0.19	0.93
1300 °C											
"water-wetted"	0.16	0.76	0.40	0.21	2.619	0.018	58.33	0.007	0.213	0.19	0.80
"dried"	0.15	0.82	0.42	0.15	2.448	0.007	68.17	0.014	0.198	0.17	0.63
1400 °C											
"water-wetted"	0.16	0.77	0.41	0.20	2.562	0.022	57.35	0.006	0.211	0.18	0.78
"dried"	0.15	0.89	0.40	0.10	2.539	0.007	61.85	0.008	0.179	0.16	0.40

As was described in [18], the component with defect-related τ_{int} lifetime can reflect positron trapping sites caused by water. Under accepted prerequisites, these extended defects can be associated with pseudogap voids at the interface between the outer surface layer of agglomerated nanoparticles and innermost layer of surrounding initial matrix (as it well demonstrated in [24, 25]). The bulk positron lifetime can now be attributed to

bulk positron lifetime of nanoparticle agglomerate. The positron trapping rate of nanoparticle-related traps κ_d can be also estimated in terms of known two-state positron trapping formalism [26].

Therefore, the defect-related lifetime τ_{int} caused by water-immersion in ceramics sintered at different T_s, remains the same as lifetime τ_2 for modified ("dry") matrix (Table II). Other values of positron trapping parameters such as $\tau_{av.}$ and τ_b, lifetimes associated with the positron annihilation in defect-free area in material and positron trapping rate in defects κ_d have not essential transformations. However, the intensity of the third component I_3 (Table I) in "immersed" ceramics is higher in order in "dry" samples. Such a result can be indicated that physical-adsorbed water fills the nanopores of ceramics, where "pick-off" annihilation of *o*-Ps in water for a "bubble" mechanism occurs (lifetime $\tau_3 \approx 1.88$ ns reflects annihilation of *o*-Ps in water) [27]. However, physical-adsorbed water does not modify positron trapping sites near grain boundaries.

In comparison with the first experiment, the second experiment was performed for MgO–Al_2O_3 ceramics immersed for 1 day in a distiller at 100% of relative humidity and finally dried ceramics in vacuum for 4 h at 120 °C (Table III). Obtained effects are described in detail in [17]. The PAL spectra were decomposed in four components, but in this work we shall focuse mainly on transformations in the second (τ_2, I_2) component.

Structure of MgO–Al_2O_3 ceramics sintered at 1100 °C, 1200 °C is still not sufficiently developed, and not all adsorbed water is desorbed (part of them clogs voids near grain boundaries). The ceramics obtained at higher temperatures of 1300 °C and 1400 °C have a developed structure of grains and pores [7, 11].

As shown in Table III, preferential decrease of the lifetime τ_2 in water-wetted MgO–Al_2O_3 ceramics and increase of their intensity I_2 demonstrates intensification of positron trapping in defects near grain boundaries filled with water (Table III). The value of defect-related lifetime τ_2 caused by desorption of water is lower than in the case of water-wetted ceramics sintered at 1100 °C (Table III). Thus, adsorbed water in ceramics sintered at lower temperature clogs part of voids near grain boundaries (sites where positrons can be trapped).

After drying, the intensities I_2 decrease in ceramics sintered at 1300 °C and 1400 °C, whereas τ_2 lifetimes are larger in ceramics prepared at 1200 °C and 1300 °C. Thus, most probably the water-adsorption processes are accompanied by agglomeration of free-volume voids near grain boundaries in MgO–Al_2O_3 ceramics at water desorption.

4. Conclusions

Water-sorption processes near grain boundaries in the modified MgO–Al_2O_3 ceramics prepared at different temperature are studied using three- and four-component treatment as well as positron–positronium trapping algorithm. Performed analysis allows to suppose that physical-adsorbed water is mainly localized in the nanopores of ceramics and practically does not penetrate into grain boundaries. The chemical-adsorbed water near grain boundaries modifies voids where positrons can be trapped. This process is accompanied by fragmentation of voids at water desorption.

Acknowledgments

H. Klym thanks the Ministry of Education and Science of Ukraine for support under Project for Young Researchers No. 0116U4411 and State Fund for Fundamental Research of Ukraine under Grant President of Ukraine.

References

[1] E. Traversa, *Sensors Actuat. B Chem.* **23**, 135 (1995).

[2] B.M. Kulwicki, *J. Am. Ceram. Soc.* **74**, 697 (1991).

[3] G. Gusmano, G. Montesperelli, E. Traversa, A. Bearzotti, G. Petrocco, A. D'amico, C. Di Natale, *Sensors Actuat. B Chem.* **7**, 460 (1992).

[4] G. Gusmano, G. Montesperelli, E. Traversa, G. Mattogno, *J. Am. Ceram. Soc.* **76**, 743 (1993).

[5] G.S. Armatas, C.E. Salmas, M.G. Louloudi, P. Androutsopoulos, P.J. Pomonis, *Langmuir* **19**, 3128 (2003).

[6] M.A. Kashi, A. Ramazani, H. Abbasian, A. Khayyatian, *Sensors Actuat. A* **174**, 69 (2012).

[7] H. Klym, A. Ingram, I. Hadzaman, O. Shpotyuk, *Ceram. Int.* **40**, 8561 (2014).

[8] H. Klym, A. Ingram, O. Shpotyuk, J. Filipecki, I. Hadzaman, *J. Phys. Conf. Ser.* **289**, 012010 (2011).

[9] H. Klym, A. Ingram, *J. Phys. Conf. Ser.* **79**, 012014 (2007).

[10] J. Filipecki, A. Ingram, H. Klym, O. Shpotyuk, M. Vakiv, *J. Phys. Conf. Ser.* **79**, 012015 (2007).

[11] H. Klym, I. Hadzaman, O. Shpotyuk, *Mater. Sci.* **21**, 92 (2014).

[12] I. Karbovnyk, I. Bolesta, I. Rovetski, S. Velgosh, H. Klym, *Mater. Sci. — Poland* **32**, 391 (2014).

[13] A. Bondarchuk, O. Shpotyuk, A. Glot, H. Klym, *Rev. Mexic. Fis.* **58**, 313 (2012).

[14] R. Golovchak, Sh. Wang, H. Jain, A. Ingram, *J. Mater. Res.* **27**, 2561 (2012).

[15] Y. Kobayashi, K. Ito, T. Oka, K. Hirata, *Radiat. Phys. Chem.* **76**, 224 (2007).

[16] R. Krause-Rehberg, H.S. Leipner, *Positron Annihilation in Semiconductors. Defect Studies*, Springer, Berlin 1999.

[17] H. Klym, A. Ingram, O. Shpotyuk, I. Hadzaman, V. Solntsev, *Nanoscale Res. Lett.* **11**, 133 (2016).

[18] O. Shpotyuk, J. Filipecki, A. Ingram, R. Golovchak, M. Vakiv, H. Klym, V. Balitska, M. Shpotyuk, A. Kozdras, *Nanoscale Res. Lett.* **10**, 77 (2015) .

[19] H. Klym, I. Hadzaman, O. Shpotyuk, M. Brunner, *Nanoscale Res. Lett.* **9**, 149 (2014).

[20] J. Kansy, *Nucl. Instrum. Methods Phys. Res. A* **374**, 235 (1996).

[21] H.I. Klym, A.I. Ivanusa, Yu.M. Kostiv, D.O. Chalyy, T.I. Tkachuk, R.B. Dunets, I.I. Vasylchyshyn, *J. Nano-Electron. Phys.* 9, 03037 (2017).

[22] P.M.G. Nambissan, C. Upadhyay, H.C. Verma, *J. Appl. Phys.* **93**, 6320 (2003).

[23] H. Klym, A. Ingram, O. Shpotyuk, L. Calvez, E. Petracovschi, B. Kulyk, R. Serkiz, R. Szatanik, *Nanoscale Res. Lett.* **10**, 49 (2015).

[24] S. Chakraverty, S. Mitra, K. Mandal, P.M.G. Nambissan, S. Chattopadhyay, *Phys. Rev. B* **71**, 024115 (2005).

[25] S. Mitra, K. Mandal, S. Sinha, P.M.G. Nambissan, S. Kumar, *J. Phys. D Appl. Phys.* **39**, 4228 (2006).

[26] Y.C. Jean, P.E. Mallon, D.M. Schrader, *Principles and Application of Positron and Positronium Chemistry*, World Sci., New Jersey 2003.

[27] I. Leifer, R.K. Patro, *Continent. Shelf Res.* **22**, 2409 (2002).